Research article

International Journal of Heterocyclic Chemistry, Vol. 9, No. 3, pp. 22-38 (summer 2019)

http://ijhc.iauahvaz.ac.ir

Green synthesis of pyranopyrazoles using Tungestic acid/Zr bio-based MOF as an efficient heterogeneous catalyst

Shima khademi[1,2], Saeed Zahmatkesh[2,3,*], Alireza Aghili[4], Rashid Badri[1,2]

[1] Department of Chemistry, Khouzestan Science & Research Branch, Islamic Azad University, Ahvaz, Iran

[2] Department of Chemistry, Ahvaz Branch, Islamic Azad University, Ahvaz, Iran

[3] Department of Science, Payame Noor University (PNU), 19395-4697, Tehran, Islamic Republic of Iran

[4] Department of Polymer Engineering, Shiraz Branch, Islamic Azad University, Shiraz, Iran

*Corresponding author. Tel.: +98 9177128745.

E-mail address: zahmatkesh1355@yahoo.com (S. Zahmatkesh)

Abstract

This reported work aims to fabricate an eco-friendly Zr bio-based MOF as a new magnetic nanocatalyst based on the immobilization of tungstic acid onto new design robust, cost-effective, green and scalable Zirconium-L-aspartate amino acid metal-organic framework (MOF)-grafted L-(+)-tartaric acid stabilized magnetite nanoparticles (Fe_3O_4/Tart-NPs) was successfully prepared by two successive hydrothermal method. This catalyst was characterized by FT-IR, XRD, FE-SEM and TGA-DTA analysis. This catalyst is outstanding to prepare l - (4 - phenyl) - 2,4 - dihydropyrano [2,3 - c] pyrazole derivatives in aqueous media due to the open metal sites, high and steady proton conductivity in the zirconium-MOF, MIP-202(Zr), MOF and also due to Brønsted acid properties of tungstic acid. This acidic catalyst can easily be extracted by an outward magnetic field after completion of the reaction without any deactivation or selectivity loss. The products were characterized by spectroscopic analysis (^{1}HNMR,^{13}CNMR and also FTIR). The optimized reaction conditions and a possible reaction mechanism is outlined.

Keywords

Tungstic acid, Nano-catalyst, Pyranopyrazole derivatives

1. Introduction

Constituting an important heterocyclic scaffold with a rich bioactive profile in medicinal chemistry, Pyranopyrazoles exhibit anticancer [1], antimicrobial [2], antioxidant [3], anti-inflammatory [4]. Besides this, they also possess DNA-binding ability [5] and potential inhibitors of cholinesterases [6,7].In the past decade, multi-component reactions (MCRs) have attracted researchers with increasing awareness to develop high atom economy, eco-friendly, one-pot, single step, energy minimized, and negligible waste production strategies. These features encourage MCRs as well-suited for the easy construction of diversified arrays of valuable bioactive heterocycles. Recently, to improve the efficiency of pyranopyrazoles and its derivatives production, several catalysts such as SO_3H@carbon powder [8], MIL-53 (Fe) metal–organic frameworks (MOFs) [9], iron-doped calcium oxalates [10], poly (ethylene imine)-modified magnetic hallo site nanotubes [11], nano-$Al_2O_3/BF_3/Fe_3O_4$ [12] have been developed. All of these catalysts suffer from several drawbacks: difficult separation from the reaction medium, high costs, low surface area, middle electronic and thermal stability, and the use of toxic organic solvents. The unique combination of magnetic nanoparticles, high surface area materials containing catalytic reactive sites such as MOFs [13] and graphene [14] and other catalytically active species such as SO_3H, Lewis acid and noble metal nanoparticles presents the opportunity to refine a range of catalyst challenges [15, 16]. For this proposes, one-pot capping, stabilizing and functionalization of Fe_3O_4 nanoparticles opens a new path for researchers which till now citric acid, ascorbic acid, tartaric acid, etc. was used for simultaneous decreasing of nanoparticles sizes [17]. Besides, due to the low surface area of Fe_3O_4 and its stabilized nanoparticles used of high surface area materials with chemical growth capability is an important issue [18, 19]. Amongst, MOFs as organic-inorganic coordinated materials have been reported as a promising class of solids for such applications [20]. Nevertheless, so far, the reported MOFs are low environmental-friendly, due to its involvement of either toxic metal ions or time and effort-consuming organic linker synthesis [21]. In this context, the design of highly surface area and biocompatible, thermal and electronic stable, robust, cost-effective, low toxicity, and scalable preparation MOF based zirconium as metal cluster and L-aspartic acid as green L-α-amino acid was developed as MIP-202 (MIP stands for the Materials of the Institute of porous materials from Paris) [21, 22]. However, these compounds themselves have moderate catalytic properties, though suitable sites for the growth of other reactive catalysts such as SO_3H, Lewis acid and noble metal nanoparticles and Brønsted acid while so far there are no reports for tungstic acid as Brønsted acid catalyst [23]. We decide to load tungstic acid (H_2WO_4. H_2O) on amino group of as-proposed MIP-202 (Zr) which benefit from high acidity, high thermal stability, and desirable hydrophobicity, in comparison with the other [24]. Briefly, in this work, we designed a new magnetic nanocatalyst based on the immobilization of tungstic acid onto Zr-L-aspartate amino acid MOF grafted L-(+)-tartaric acid stabilized Fe_3O_4 NPs and characterized by FT-IR, XRD, FESEM and TGA-DTA analysis. This heterogeneous catalyst was applied for the preparation of biologically potent l-(4-phenyl)-2,4-dihydropyrano[2,3-c] pyrazole derivatives in aqueous media via multicomponent reactions (Scheme 1) [25]. The catalytically synthesized derivatives were

confirmed by ^{1}HNMR and ^{13}CNMR and FTIR analysis. Possible reaction mechanisms and optimize conditions for the l-4-phenyl-2,4-dihydropyrano[2,3-c]pyrazole derivatives preparation were outlined.

2. Experimental section

2.1. General information

All required chemicals were purchased from commercial suppliers and used without any further purification. Tartaric acid (Tart), iron(III) chloride hexahydrate ($FeCl_3 \cdot 6H_2O$), L-(+)-tartaric acid, urea, diethylene glycol, ethanol, zirconium chloride ($ZrCl_4$), L-aspartate (LA) amino acid, sodium tungstate dihydrate ($Na_2WO_4.2H_2O$), n-hexane, HCl, malononitrile and ethyl acetoacetate and other compound were purchased from different commercial sources (Sigma-Aldrich and Merck Company). Double distilled water was used for the entire synthesis. Reactions were monitored by TLC using silica gel 60 F254 coated aluminum sheets with ethyl acetate/hexane (3:7) mixture as the eluting medium. Melting points are uncorrected and were determined using an Electrothermal apparatus by the open capillary method. FT-IR spectra were recorded on a JASCO-680 instrument (Jasco Company, Tokyo, Japan) using KBr optics. X-ray diffraction (XRD) pattern was tested by an automated Philips X'Pert X-ray diffractometer from Netherlands (40 kV and 30 mA). Morphological analysis was investigated by field-emission scanning electron microscopy (FE-SEM, ZEISS SUPRATM 50 VP, Germany.TGA measurements were recorded by DTG-60 Shimadzu instrument. NMR spectra were recorded on a BRUKER AVANCE III HD Nanobay 400 MHz spectrometer in DMSO-d_6, and δ values are expressed in ppm using TMS as an internal standard.

2.2. General procedure

2.2.1. Synthesis of Fe_3O_4

Magnetic Fe_3O_4 particles were synthesized based on a modified co-precipitation method.[28-30] Briefly, the mixture of $FeCl_3.6H_2O$ (1.3 g, 4.8 mmol), $FeCl_2.4H_2O$ (0.9 g, 4.5 mmol) and polyvinyl alcohol (PVA 15000) (1 g) as a surfactant was dissolved in water (30 mL) with vigorous stirring. Afterwards, as the temperature of the mixture was elevated to 80 ^{o}C, a proper amount of hexamethylenetetramine (HMTA) (1.0 mol/L) was added dropwise until reaction media reaches pH 10. The black magnetic particles were collected with the help of a magnetic filed, followed by washing with ethanol and deionized water three times. The product was then dried at 80 ^{o}C for 10 h.

2.2.2. Synthesis of Fe_3O_4/Tart-NPs

Fe_3O_4 nanoparticles (NPs) stabilized with chiral tartaric acid (Tart) was synthesized as follows: typically, $FeCl_3 \cdot 6H_2O$ (0.81 g, 3 mmol), L-(+)-tartaric acid (0.075 g, 0.5 mmol) and urea (1.80 g, 30 mmol) were completely dissolved in diethylene glycol (30 mL) by vigorous mechanical stirring. The obtained solution was sealed in a Teflon lined stainless steel autoclave and then heated at 200 °C for 8 h. After cooling to room temperature, the black magnetite was separated magnetically and washed with ethanol several times to eliminate organic and inorganic impurities, and then dried at 60 °C for 6 h.

2.2.3. Fe_3O_4/Tart-MIP-202

Fe_3O_4/Tart-MIP-202 was synthesized as follows: typically, 0.25 g of Fe_3O_4/Tart was dispersed in 10 mL deionized water under ultrasound irradiation for 2 h. A mixture of $ZrCl_4$ (1.15 g, 4.93 mmol)
and L-aspartate (LA) amino acid (1.4 g, 10.52 mmol) was completely dissolved in 10 mL deionized water and added in Fe_3O_4/Tart suspension. Subsequently, the solution was transferred into a Teflon lined stainless steel autoclave and then heated at 120 °C for 24 h. After cooling down to room temperature, the resulting precipitate was isolated by an external magnet and washed with EtOH for several times. After that, the precipitate was immersed in EtOH (80 mL) for 12 h, during which EtOH was refreshed every 3 h. Finally, the precipitated powder was collected by an external magnet and dried in a vacuum oven at room temperature for 24 h.

2.2.4. Fe_3O_4/Tart-MIP-202-Tungstic acid (H_4WO_5)

Tungstic acid-functionalized Fe_3O_4/Tart-MIP-202 was prepared by reaction with Fe_3O_4/Tart-MIP-202 and sodium tungstate dihydrate. 0.5 g of Fe_3O_4/Tart-MIP-202 in 15 mL n-hexane was placed in a 50 mL round bottom flask. Then 0.658 g of sodium tungstate dihydrate was added to the dispersed Fe_3O_4/Tart-MIP-202 solution and then it was refluxed for 12 h under a nitrogen atmosphere. After completion of the reaction it was cooled to room temperature and filtered through suction followed by washing thoroughly with n-hexane (10 mL) and distilled water (10 mL), respectively. The sample was dried and then stirred in the presence of a 15 mL aqueous HCl medium so that the pH of the solution comes down to ca. 4.0 in 1 h. Finally, the mixture was filtered, washed with distilled water and dried at room temperature.

2.2.5. General procedure for the preparation of l-(4-phenyl)-2,4- dihydropyrano[2,3-c] pyrazole derivatives

To a mixture of an aromatic aldehyde (1 mmol), malononitrile (1 mmol), ethyl acetoacetate (1 mmol) and hydrazine hydrate (1 mmol) in a round bottom flask, 40 mg of Fe_3O_4/MIP-202-H_4WO_5 was added and the resulting mixture was vigorously stirred long enough in water solvent at 60 ℃.(scheme1.) After completion of the reaction as observed by TLC (n-hexane/ethyl acetate: 7/3), the catalyst was separated magnetically. The Fe_3O_4/MIP-202-H_4WO_5 was washed with ethanol and then dried at 50 ℃ for 3 h in order to preserve catalyst and it was used for the alternative reaction. Subsequently, the products in the aqueous layer was filtered, separated and then the crude product was purified by washing with acetone. The purity of products were studied by TLC and ^{1}H-NMR, ^{13}C-NMR and FT-IR spectroscopy

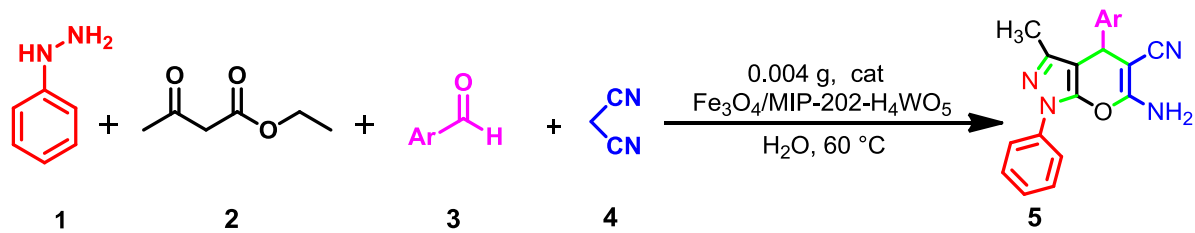

Scheme 1. Synthesis of dihydropyrano[2,3c]pyrazoles using Fe_3O_4/MIP-202-H_4WO_5

2.2.5.1. Spectral data for selected synthesized 6-Amino-3-methyl-4-(2,4-dicholorophenyl)-1-phenyl-1,4-dihydropyrano[2,3-c]pyrazole-5-carbonitrile catalyzed by Fe3O4/MIP-202-H4WO5

White powder,IR (KBr, cm-1): 3455, 3332 (NH2), 3056 (=C-H), 2954 (C-H), 2193 (CN), 1574, 1482 (C=C), 1130 (C-O), 752; ^{1}H-NMR (400 MHz, DMSO-d6,): δ(ppm):1.79 (s, 3H), 5.16 (s, 1H), 7.32-7.35 (d, 3H, J=8.0 Hz), 7.38-7.39 (d, 1H), 7.43-7.44 (d, 1H), 7.49-7.52 (t, 2H, J=8.0 Hz), 7.56 (s, 1H), 7.63 (s, 1H), 7.80 (s, 2H).
^{13}C-NMR (100 MHz, DMSO-d6): δ(ppm): 12.82, 56.67, 97.77, 119.98, 120.53, 126.76, 128.58, 129.42, 129.81, 132.96, 133.00, 133.56, 137.91, 144.75, 145.30, 145.30, 160.41.

2.3. Antimicrobial screening

2.3.1. Antimicrobial activity of synthesized compounds by disc diffusion test

Antimicrobial activities of the synthesized compounds were evaluated against Staphylococcus aureus (S. aureus), Escherichia coli, methicillin resistance Staphylococcus aureus (MRSA) Pseudomonas auroginosa and Candida albicans. Antibacterial activities of synthesized compounds detected by disc diffusion method and minimum inhibitory concentration (MIC) was used. Primary all of the bacterial isolates and candida albicans cultured on Mueller Hinton agar (Merck, UK). These bacteria and candida albicans were seeded in Mueller Hinton agar by the pour plate technique. Diameter paper discs with of each of the compounds (0.9% w/v) and methanol (as control) was applied to the agar plates and incubated at 37 _C or 46 h. The formation of an inhibition zone around the disc is an indication of antibacterial activity [35].

2.3.2. Determination of the minimum inhibitory concentration (MIC) of synthesized compounds

Lowest concentration of an antibacterial agent which prevents the growth of a microorganism defined as minimum inhibitory concentration (MIC), and was determined in 96-well microtiter plates according published in guidelines. E. coli, S. aureus, MRSA,P. auroginosa and C. albicans were cultured overnight in cation-adjusted Mueller Hinton Broth (MHB) at 37 _C and used to a final density of 8 log colony forming units (CFU)/mL. Gradient concentrations of synthesized compounds were added to MHB. Bacteria/synthesized compounds mixed cultures were evaluated using a microplate reader at 37 _C on a rotary shaker at 200 rpm. Optical density (OD) at 600 nm was determined for bacterial cell growth in all samples. Each experiment was performed in triplicate [36,37].

3. Results and discussion

3.1. Characterization of as-prepared samples

The Fe_3O_4/MIP-202-H_4WO_5 material was in nano-sized amorphous and it can be more effective as a catalyst due to the large acidic density of H_4WO_5 groups presented in the high surface area of Fe_3O_4/MIP-202 surface. Our part of interest was in exploring the catalytic activity of

Fe_3O_4/MIP-202-H_4WO_5 for the preparation of l-(4-phenyl)-2,4- dihydropyrano[2,3-c] pyrazole derivatives in aqueous media via multicomponent reactions. This catalyst was characterized by FT-IR, XRD, FE-SEM and TGA-DTA analysis.

The FT-IR spectra of the Fe_3O_4 (as-comparison), Fe_3O_4/Tart, MIP-202(Zr), Fe_3O_4-MIP-202(Zr), and Fe_3O_4/MIP-202-H_4WO_5 samples are shown in Fig. 1. The Fe_3O_4 nanoparticles spectrum shows two broad peaks at 1600 cm^{-1} and 3365 cm^{-1} attributed to O–H bending and stretching mode of Fe–OH, respectively. The characteristic lattice vibration of the magnetite peak for Fe–O band was observed at 560 cm^{-1} (Fig. 1a). In Fe_3O_4/Tart spectrum, a dominant peak at 1730 cm^{-1}, resulting from the carbonyl stretch (C=O) associated with protonated carboxyl groups, which confirmed adsorption/chemisorption of tartaric acid on Fe_3O_4 NPS as the carboxyl groups. The appeared peaks at 1550 cm^{-1} and 1420 cm^{-1} represent the asymmetric and symmetric COO carbon–oxygen stretches of carboxylate groups, respectively [17]. Results confirmed that Tart as a monotartrate species was chemisorbed on the Fe_3O_4-NPs surface as a carboxylate as reactive organic cross-linker for MOF grafting. The FTIR spectrum of MIP-202 (Zr) MOF (Fig. 1c) displays vibration mode at 660 cm^{-1} and 470 cm^{-1} which is due to stretching vibrations of the Zr-OH and Zr-COO frameworks. Whereas the small band at 530 cm^{-1} is ascribed to Zr-(OC) asymmetric stretching vibrations. Bands indicating the occurrence of asymmetric and symmetric (OCO) stretching's in the linker are visible at 1550 cm^{-1} and 1420 cm^{-1}, respectively. Absence of free–COOH groups in 1673 cm^{-1} implies successful coordination of Zr to COO group and makes the MIP-202(Zr) (Fig. 1c). When Fe_3O_4-MIP-202(Zr) nanostructures were synthesized, the position of absorption bands of Fe_3O_4/Tart nanoparticle, and MIP-202(Zr) nanostructure in the final structure (Fig. 1d) don't change, which confirmed the successful formation of Fe_3O_4-MIP-202(Zr) sample (Fig. 1d) as well as not appeared no new peak. The presence of Tart on Fe_3O_4-NPs help the formation of the same Zr-O-C complex on the Fe_3O_4 surface and grafted by L-aspartic acid for better construction of MIP-202(Zr) MOF. After H_4WO_5 loading, corresponded FTIR spectra show the characteristic peak of W-O species in the range of 800-960 cm^{-1}, as well as the characteristic bands of other parts of composite was stable and appeared at final FTIR spectrum (Fig. 1e).

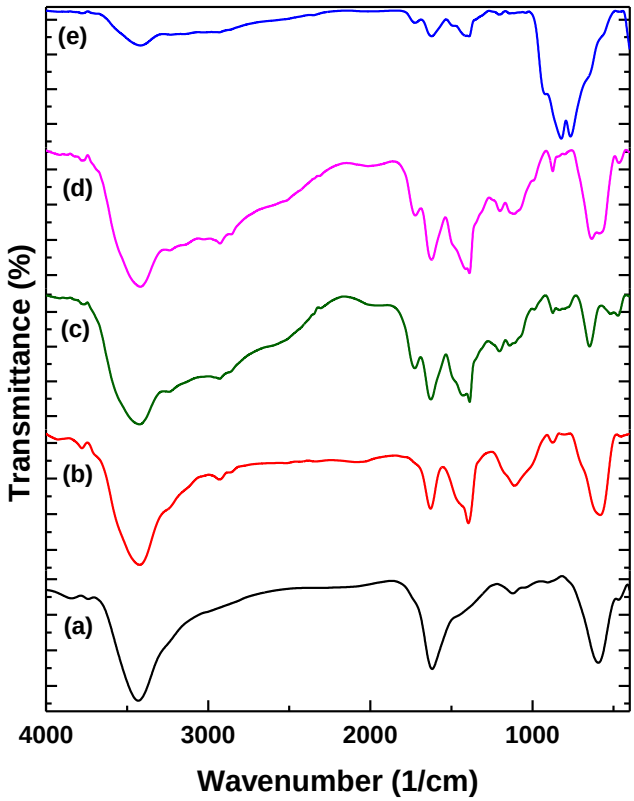

Fig. 1. FT-IR spectra of Fe_3O_4 nanoparticles (a), Fe_3O_4/Tart (b), MIP-202(Zr) (C), Fe_3O_4-MIP-202(Zr) (d) and Fe_3O_4/MIP-202-H_4WO_5 (e) samples

The crystallinity of the as-prepared samples was recorded by wide angle X-ray powder diffraction (XRD). The XRD patterns of Fe_3O_4 (Fig. 2a) shows six characteristic peaks at 2θ of 30.3°, 35.4°, 43.2°, 53.5°, 57.2° and 62.9° corresponding to the (220), (311), (400), (422), (511) and (440) crystal planes of cubic inverse spinel. When Fe_3O_4 was synthesized in the presence of L-tartaric acid, the intensity of the as mention peaks decreases while the positions of all diffraction peaks for both Fe_3O_4-NPs and Fe_3O_4/Tart-NPs well match (Fig. 2b) [17]. XRD pattern of as-synthesized MIP-202(Zr) MOF is identical to the simulated XRD results calculated based on single-crystal structure for MIP-202 as well as confirms the high phase purity [23]. After MOF grafting on Fe_3O_4-Tart NPs, no appearance of new peaks while correspond MIP-202 and Fe_3O_4-NPs peaks. After H_4WO_5 loading on high surface area of Fe_3O_4/MIP-202 the corresponded XRD pattern in addition to the MIP-202 and Fe_3O_4 peaks show new diffraction peaks related to those in the standard database (PDF: 00-018-1420) of H_4WO_5 (Fig. 2)[26].

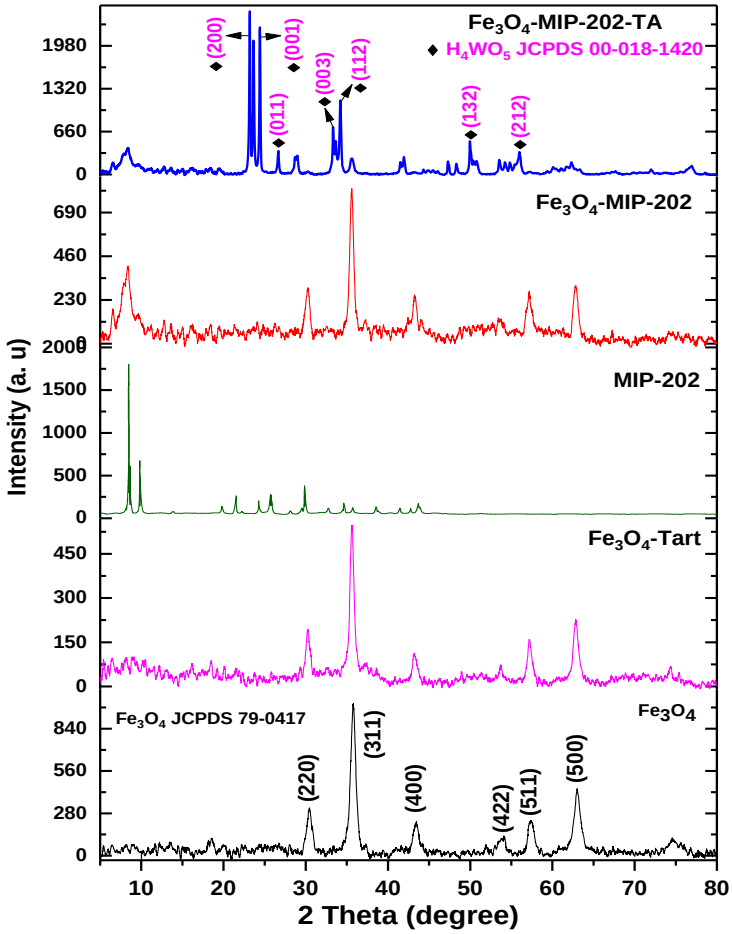

Fig. 2. XRD patterns of Fe_3O_4 nanoparticles, Fe_3O_4/Tart, MIP-202(Zr), Fe_3O_4-MIP-202(Zr) and Fe_3O_4/MIP-202-H_4WO_5 samples

The size, shape and size distribution of the Fe_3O_4/Tart, MIP-202(Zr), Fe_3O_4-MIP-202(Zr) and Fe_3O_4/MIP-202-H_4WO_5 were examined by FESEM technique (Fig. 3). The FESEM images of Fe_3O_4/Tart (Fig. 3a) show that in the presence of L-(+)-tartaric acid the Fe_3O_4 particles have a uniform smooth spherical shape in nanosize distribution. The carboxylic acid as stabilizing and capping agent causes to the becoming uniform and dramatically reducing its diameter. For comparison, pure MIP-202(Zr) was synthesised in the absence of Fe_3O_4/Tart and the FESEM images (Fig. 3b) apparent that, it had clean and smooth surface sheets which were nicely interlinked through thin and delicate three-dimensional networks, resulting in a porous, loose sponge-like structure. While after MIP-202(Zr) MOF grafted on Fe_3O_4/Tart, the corresponded FESEM image (Fig. 3d) clearly indicates the growth of MIP-202(Zr) MOF on Fe_3O_4/Tart surface. Finally, smooth and uniform cubic shapes of H_4WO_5 in the presence of Fe_3O_4-MIP-202(Zr) clearly visible and confirms the successful preparation of Fe_3O_4/MIP-202-H_4WO_5 catalyst by self-assembly and grafting reactions.

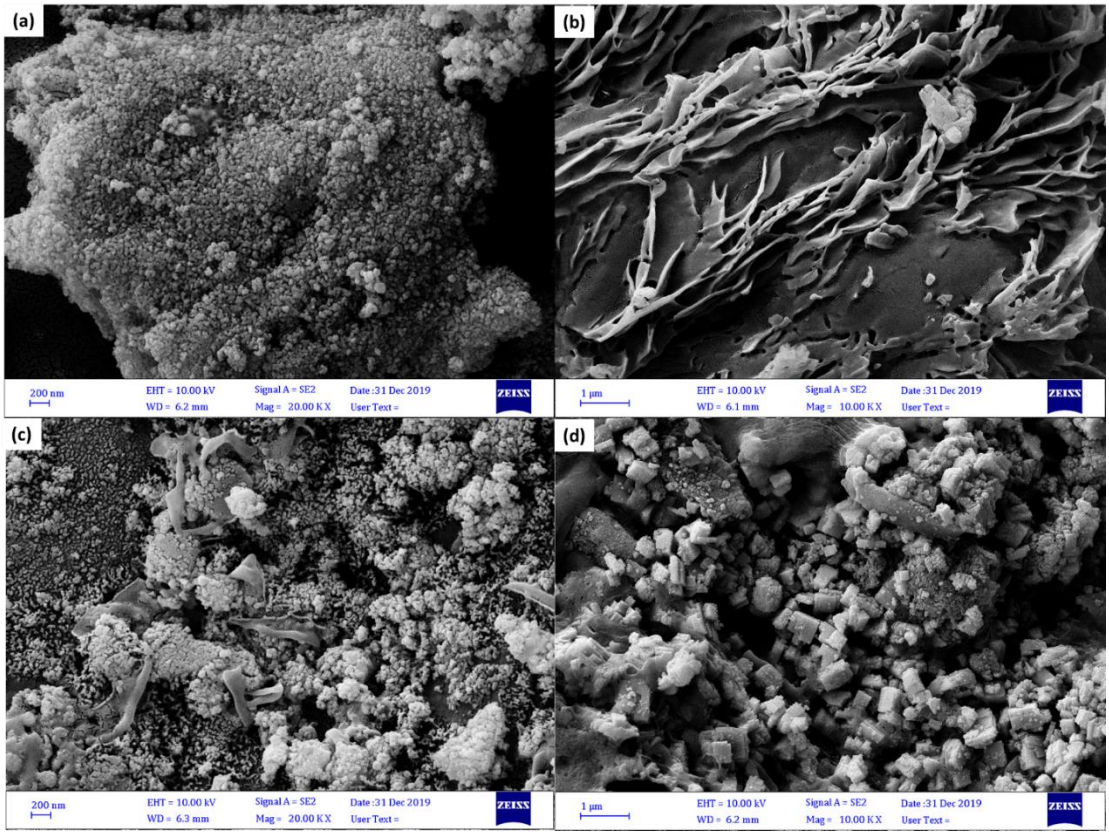

Fig. 3. The FESEM image of Fe_3O_4/Tart (a), MIP-202(Zr) (b), Fe_3O_4-MIP-202(Zr) (c) and Fe_3O_4-MIP-202(Zr)-H_4WO_5 (d) samples

DTA-DTG analysis (Fig. 4a) shows three lose weight which the first is the peak between at 35°C and 160 °C with a maximum at 95 °C attributed to the surface adsorbed of distilled water and another solvent on Fe_3O_4/MIP-202-H_4WO_5 structure. The second peak ranges between 195 °C and 320 °C with a maximum at 220 °C is related to the Tartaric acid group on the Fe_3O_4 surface. The third peak occurred between 460 °C and 610 °C with a maximum at 585 °C which is corresponded to the losing of L-aspartic acid in MIP-202 (Zr) structure while H_4WO_5 complexation with NH_2 group of L-aspartic acid will cause the more stability of MIP-202 (Zr). The thermal stability of the Fe_3O_4/MIP-202-H_4WO_5 catalyst is assertively well in the range of 0–420 °C, which covers the temperature range for the synthesis of l-(4-phenyl)-2,4-dihydropyrano[2,3-c] pyrazole derivatives.

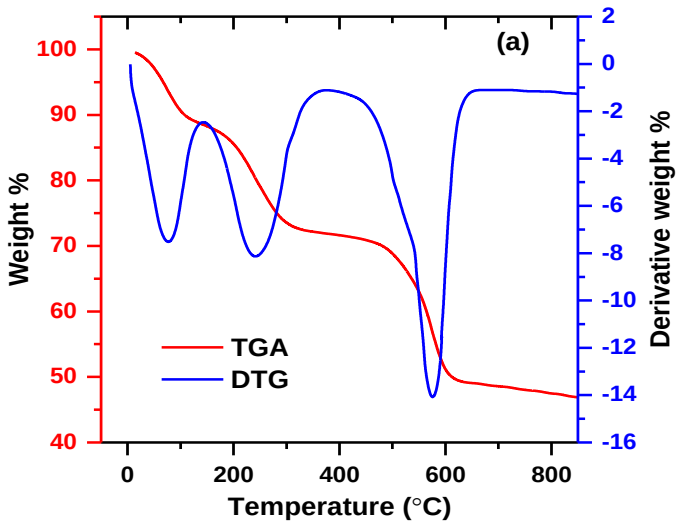

Fig.4. Thermal analysis TGA-DTA of Fe_3O_4/MIP-202-H_4WO_5 sample

According to results of disk diffusion antimicrobial test among synthesized heterocyclic compounds only three compounds have substituted (4-Br), (4-F) and (2,4-Cl) it has antimicrobial activity on S. aureus and none of the synthesized compounds on antimicrobial effect did not on gram-negative bacteria and fungi.

Due to diagonals size in lack of bacterial growth was observed in various combinations that combined have Br substituted compound of two other diagonals in lack of growth is greater in 17 mm size MIC results is also Table 4. MIC test is specified that compounds substituted Br with mount MIC = 25 ration to two other compound at lower concentrations prevent growth of bacteria

S. aureus. Two other combination MIC, which is equal with 50 athigher concentrations prevent the growth of bacteria. According to results of specified antimicrobial tests that antibacterial active 4-Br compound is more robust than other two compound and in smaller amounts can have a greater antibacterial effect. In Nasrollahi et al., study reported the resistance to gram negative and positive bacteria to synthesized heterocyclic compounds 1,4-dihydropyridines except S. aureus that susceptible to synthesized compounds [38]. On the other hands, in Mehta's study on antimicrobial activity against Gram negative and positive bacteria of some derivatives of 1,4-dihydropyridines (compounds V-1 to V-9) described. In this study, compound V-2 was effective against E. coli and nonlactose fermenters (NLF) .Compound V-3 was effective against Klebsiella aerogenes and S. aureus and compounds V-1 and V-4 were only effective against E. coli and NLF [39].

Table 4. Anti-bacterial activity of compounds against S. aureus strain (ATCC 25923).

Compd No.	R	MIC (mg/ml) Zone of inhibition (mm)	S. aureus S. aureus
7	4-Br	25	17
10	4-F	50	14
6	2,4-Cl	50	13

3.2. Catalytic activity and optimization

A typical reaction model for dihydropyrano[2,3c]pyrazoles derivatives synthesis via a multi-component reaction of ethyl acetoacetate, phenylhydrazine, malononitrile,and an aldehyde, in distilled water at 60 °C in the presence of Fe_3O_4/MIP-202-H_4WO_5 is illustrated in Scheme 1.To optimize the reaction conditions, the reaction of ethyl acetoacetate, phenylhydrazine, malononitrile and benzaldehyde, was selected and the effect of various parameters such as temperature, Fe_3O_4/MIP-202-H_4WO_5 catalyst mass and solvent type was investigated and optimized (See Table 1). In order to, the reaction was performed in the presence of varying amounts of catalyst from 0.003 g to 0.006 g and in the absence of the catalyst, this reaction takes a long time (210 min) and this indicates that the presence of Fe_3O_4/MIP-202-H_4WO_5 heterogeneous acidic catalyst is not preventable for this reaction and 0.002 g of Fe_3O_4/MIP-202-H_4WO_5 was selected as desirable mass. In higher of Fe_3O_4/MIP-202-H_4WO_5 nanocatalyst mass, no increase in yield is seen because of agglomeration of catalyst particles. Also, the efficiency and condensation reaction speed was decreased with decreasing in the catalyst mass which is due to the not available of desired number of active catalyst sites.

To determine the best reaction conditions, we have carried out the condensation reaction in the solvent free and in the presence of various solvents it can be seen in Table 1. According to the Table 1 in H_2O as solvent, high yield of product was obtained due to the better dispersion of Fe_3O_4/MIP-202-H_4WO_5 nanocatalyst than others.

The reaction temperature was also studied for selecting the appropriate temperature of reaction, 25, 50, 60, 65, 70 and 90 °C, and the results showed that the best yield is seen at 60 °C, which is due to the well dispersion and mass transfer rate in reaction section for migrating and transferring on Fe_3O_4/MIP-202-H_4WO_5. Attractively, establishing the same conditions as above (60 °C, H_2O solvent, 0.004 g of Fe_3O_4/MIP-202-H_4WO_5 catalyst) gave best yield at a shorter time, 45 min (Table 1, entries 5).

TABLE 1. Optimization of conditions in the synthesis of dihydropyrano[2,3c]pyrazoles

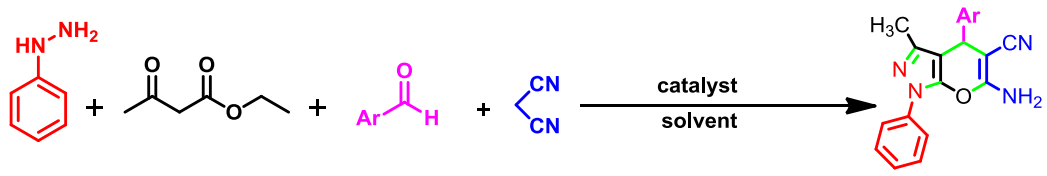

1 2 3 4 5

Entry	Solvent	Catalyst (g)	T (°C)	Time (min)	Yield [%]
1	EtOH/H_2O (1:1)	0.005	r.t	90	50
2	EtOH/H_2O (2:1)	0.005	65	60	75
3	H_2O	-	70	210	55
4	H_2O	0.005	70	50	80
5	**H_2O**	**0.004**	**60**	**45**	**92**
6	H_2O	0.003	50	55	83
7	CH_2Cl_2	0.004	Reflux	230	40

8	CCl_4	0.004	Reflux	230	42
9	$CHCl_3$	0.004	Reflux	65	40
10	THF	0.004	Reflux	65	47
11	CH_3CN	0.004	Reflux	55	53
12	MeOH	0.004	Reflux	50	60
13	EtOH	0.004	90	48	47
14	EtOH	0.004	Reflux	50	70
15	EtOH/H_2O (1:1)	0.006	r.t	60	70
16	EtOH/H_2O (1:1)	0.004	Reflux	60	75
17	EtOH/H_2O (1:2)	0.004	Reflux	50	85
18	-	0.004	Reflux	65	68
19	-	0.004	60	60	75

[a]Reaction condition: ethyl acetoacetate (1 mmol), phenylhydrazine (1 mmol), malononitrile (1 mmol), and a solvent. Catalyst: Fe_3O_4/MIP-202-H_4WO_5.

After than at optimized condition, some of the dihydropyrano[2,3c]pyrazoles derivatives were prepared in presence of different aldehydes with electron-donating or electron-withdrawing groups. Results indicate that the excellent yields for all aldehydes were obtained in short reaction times, so it can be said that this method is applicable in the presence of both electron-donating and electron-withdrawing groups (Table 2). This means that position and substitution type does not have any effect on the reaction process which shows very good and effective performance of new Fe_3O_4/MIP-202-H_4WO_5 catalyst in the synthesis of dihydropyrano[2,3c]pyrazoles derivatives.

TABLE 2. Preparation of dihydropyrano[2,3c]pyrazoles derivatives in the presence of Fe_3O_4/MIP-202-H_4WO_5 with diffrent aldehydes

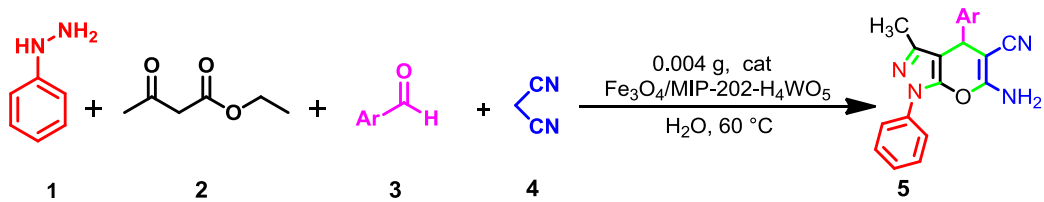

1 2 3 4 5

Entry	Ar	Product	Time (min)	Yield[a] (%)	Mp(°C)	
					Found	Reported
1	C_6H_5	**5a**	45	92	167-169	165-167 [27]
2	4-OMe-C_6H_5	**5b**	38	90	169-171	171-172 [28]
3	4-Me-C_6H_4	**5f**	40	89	173-175	176-178 [29]
4	3-OEt-4-OH-C_6H_4	**5g**	55	86	166-169	170-171

						[30]
5	2-Cl-C_6H_4	**5c**	40	91	143-145	145-146 [28]
6	**2,4-Cl_2-C_6H_4**	**5d**	**35**	**92**	**181-183**	**182-184** [29]
7	4-Br-C_6H_4	**6e**	45	89	164-166	163-165 [30]
8	4-CN-C_6H_4	**5i**	45	90	194-196	197-199 [29]
9	4-benzyloxy-C_6H_4	**5h**	40	92	163-166	162-164 [30]
10	4-F-C_6H_4	**5k**	40	91	191-193	194-196 [30]
11	3-NO_2-C_6H_4	**5j**	40	92	189-191	188-190 [30]
[a]Reaction condition: Ethyl acetoacetate (1 mmol), phenylhydrazine (1 mmol), malononitrile (1 mmol), and H_2O. Catalyst mass: Fe_3O_4/MIP-202-H_4WO_5 (0.004 g).						

3.4. Proposed Mechanism

A possible mechanism for the synthesis of dihydropyrano [2,3c] pyrazoles is shown in Scheme 4. In this mechanism, the role of Fe_3O_4/MIP-202-H_4WO_5 as an acidic catalyst is showing in electrophilic activation for nucleophilic attack of amino group. Fe_3O_4/MIP-202-H_4WO_5 as an acidic catalyst initially activates malononitrile for nucleophilic attack while the presence of an Fe_3O_4/MIP-202-H_4WO_5 as acidic catalyst in the enol-keto equilibrium in 3-methyl-1-phenyl-5-pyrazolone **8** is furthered in the form of analysis, which then undergoes activated Michael addition to the Knoevenagel product formed between aldehydes and malononitrile. Finally, intramolecular nucleophilic cyclization and tautomerization afford the 1,4-dihydropyrano [2,3-c]pyrazoles. **(Scheme 2)**

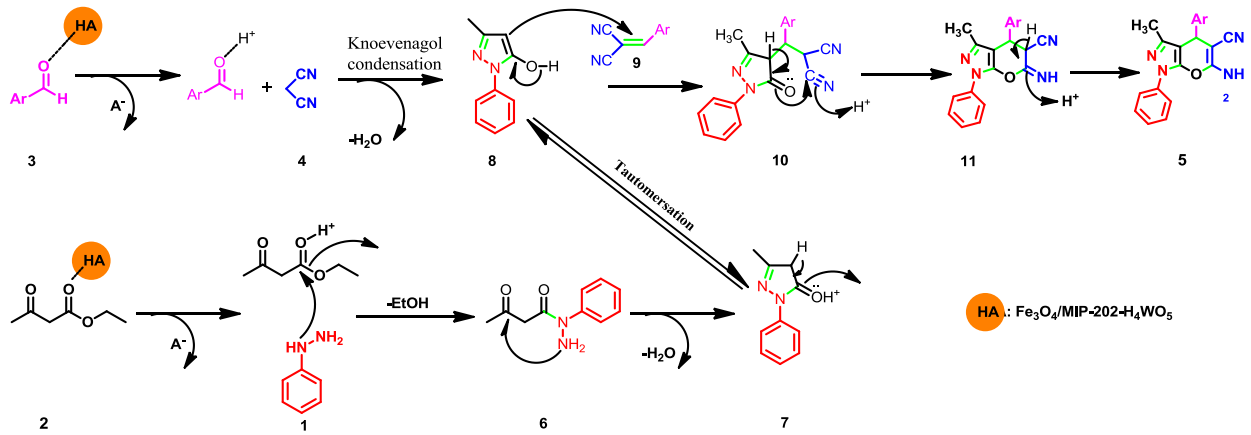

Scheme 2. The suggested mechanism for the catalyzed synthesis of 1,4-dihydropyrano [2,3c]pyrazole using Fe_3O_4/MIP-202-H_4WO_5

3.5. Reusability of Catalyst

The recovery test is a simple and easy method to prove the performance of a magnetite separable catalyst. for this purpose, after separating the Fe_3O_4/MIP-202-H_4WO_5 catalyst by external magnet it was washed several times with H_2O or ethanol, and dried at 50 °C. The recovered Fe_3O_4/MIP-202-H_4WO_5 was used 6 cycles for 1,4-dihydropyrano [2,3c]pyrazole preparation at optimized conditions in which the results showed not-significant variation in reaction yields due to the high electric, thermal and chemical stability of Fe_3O_4/MIP-202-H_4WO_5 catalyst (Fig. 5).

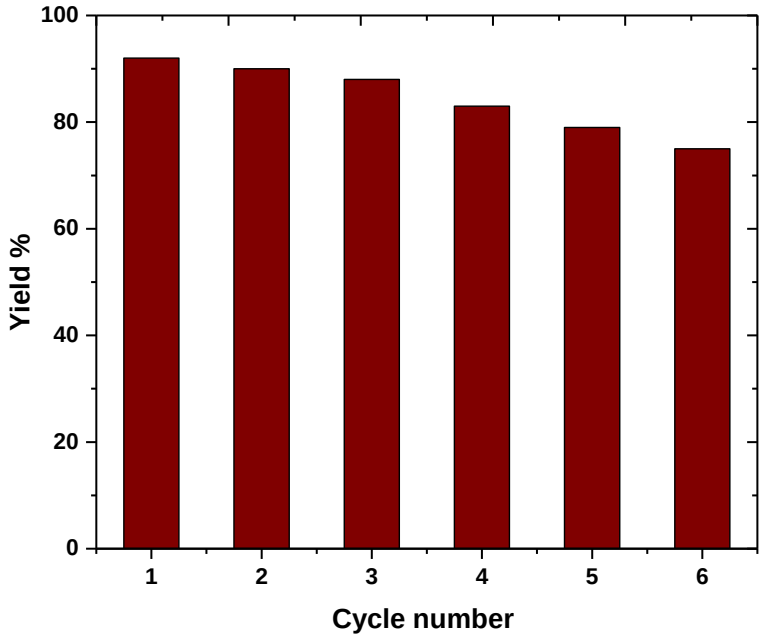

Fig. 5. The reusability Fe_3O_4/MIP-202-H_4WO_5 samples

3.6. Comparison whit literature

The comparison of our proposed catalyst efficiency for synthesis of 1,4-dihydropyrano [2,3c]pyrazoles with other reported catalysts was also evaluated (Table 3). Results showed that Fe_3O_4/MIP-202-H_4WO_5 has much higher catalytic reactivity than others in terms of reaction temperature, product yield, reaction time, and catalyst reusability which are due to the satisfactory surface area and surface charge of as-prepared catalyst and also it was thermal and chemical stable.

TABLE 3. Comparison of Fe_3O_4/MIP-202-H_4WO_5 with other catalysts reported in the literature for the synthesis of dihydropyrano[2,3c]pyrazole

Entry	Catalyst	Conditions	Time (min)	Yield (%)	Ref
1	$InCl_3$ (10 mol %)	EtOH-H_2O (2: 1), reflux	150	91	[31]
2	γ-alumina (30 mol %)	H_2O, reflux	50	80	[32]
3	Sodium benzoate (15 mol %)	Water, r.t.	60	85	[33]
4	$H_{14}[NaP_5W_{30}O_{110}]$ (1 mol %)	H_2O, reflux	60	94	[34]
5	**Fe_3O_4/MIP-202-H_4WO_5 (0.004 g)**	**H_2O solvent, 60 °C**	**45**	**92**	**This work**

4. Conclusion

In summary, we have successfully demonstrated a green route for the one-pot four-component synthesis of pyranopyrazole under a aqueous medium using a Zr bio-based MOF , which is stabilized on magnetite nanoparticles was successfully prepared. fully characterized and subsequently applied as an effective heterogeneous, robust, cost-effective, green, chemical, thermal and electronic stable, and scalable catalyst for the synthesis of l-(4-phenyl)-2,4-dihydropyrano[2,3-c]pyrazole derivatives by one-pot condensation reaction. This method benefits from clean work-up and easy reusability of the catalyst, satisfactory reaction time, and high efficiency under distilled water as green media. It is expected that this catalyst and proposed method would be extensively used in the combinatorial chemistry, diversity-oriented organic synthesis, and drug discovery while this catalyst can be used in photocatalytic system for ORR and water splitting reactions. From these studies we can conclude that these compounds exhibited main to moderate activities against S. aureus and can be useful in the medical field and biomedical applications.

Acknowledgements

This work was supported by Ahvaz branch of Islamic Azad University of Iran.

References

[1]Vasava, M.S.; Bhoi, M.N.; Rathwa, S.K.; Shetty, S.S.; Patel, R.D.; Rajani, D.P.; Rajani, S.D.; Patel, A.; Pandya, H.A.; Patel, H.D. Novel 1, 4-dihydropyrano [2, 3-c] pyrazole derivatives: Synthesis, characterization, biological evaluation and in silico study. J. Mol. Stru. 2019, 1181, 383-402, https://doi.org/10.1016/j.molstruc.2018.12.053.

[2]Reddy, G.M.; Sravya, G.; Yuvaraja, G.; Camilo, A.; Zyryanov, G.V.; Garcia, J.R. Highly functionalized pyranopyrazoles: synthesis, antimicrobial activity, simulation studies and their structure activity relationships (SARs). Res. Chem. Int. 2018, 44, 7491-7507, https://doi.org/10.1007/s11164-018-3569-8.

[3]Silva, V.L.; Elguero, J.; Silva, A.M. Current progress on antioxidants incorporating the pyrazole core. Eur. J. Med. Chem. 2018, 156, 394-429, https://doi.org/10.1016/j.ejmech.2018.07.007.
[4]Chavan, R.R.; Hosamani, K.M. Microwave-assisted synthesis, computational studies and antibacterial/anti-inflammatory activities of compounds based on coumarin-pyrazole hybrid. Royal Soc. Open Sci. 2018, 5, https://doi.org/10.1098/rsos.172435.
[5]Badr, M.H.; Abd El Razik, H.A. 1, 4-Disubstituted-5-hydroxy-3-methylpyrazoles and some derived ring systems as cytotoxic and DNA binding agents. Synthesis, in vitro biological evaluation and in silico ADME study. Med. Chem. Res. 2018, 27, 442-457, https://doi.org/10.1007/s00044-017-2071-y.
[6]Derabli, C.; Boualia, I.; Abdelwahab, A.B.; Boulcina, R.; Bensouici, C.; Kirsch, G.; Debache, A. A cascade synthesis, in vitro cholinesterases inhibitory activity and docking studies of novel Tacrine-pyranopyrazole derivatives. Bioorg. & Med. Chem. Lett. 2018, 28, 2481-2484, https://doi.org/10.1016/j.bmcl.2018.05.063.
[7]Mamaghani, M.; Nia, R.H. A Review on the recent multi-component synthesis of pyranopyrazoles.Polycyclic Aromatic Compounds 2019, 1-69, https://doi.org/10.1080/10406638.2019.1584576.
[8] N. Nagasundaram, M. Kokila, P. Sivaguru, R. Santhosh, A. Lalitha, Advanced Powder Technology, 2020[9] M.A. Ghasemzadeh, B. Mirhosseini-Eshkevari, M.H. Abdollahi-Basir, Applied Organometallic Chemistry, 2019, 33, e4679.

[10] K.K. Gangu, S. Maddila, S.N. Maddila, S.B. Jonnalagadda, RSC advances, 2017, 7, 423.
[11] Z. Hajizadeh, A. Maleki, Molecular Catalysis, 2018, 460, 87-93.
[12] E. Babaei, B.B.F. Mirjalili, Inorganic and Nano-Metal Chemistry, 2020, 50, 16.
[13] B. An, K. Cheng, C. Wang, Y. Wang, W. Lin, ACS Catalysis, 2016, 6, 3610.
[14] M. Zhang, Y.-H. Liu, Z.-R. Shang, H.-C. Hu, Z.-H. Zhang, Catalysis Communications, 2017, 88, 39.
[15] H. Niu, Y. Zheng, S. Wang, L. Zhao, S. Yang, Y. Cai, Journal of hazardous materials, 2018, 346, 174.
[16] F. Bonyasi, M. Hekmati, H. Veisi, Journal of colloid and interface science, 2017, 496, 177.
[17] L. Hadian-Dehkordi, H. Hosseini-Monfared, Green Chemistry, 2016, 18, 497.
[18] M.X. Wu, J. Gao, F. Wang, J. Yang, N. Song, X. Jin, P. Mi, J. Tian, J. Luo, F. Liang, Small, 2018, 14, 1704440.
[19] J. Liu, F. Yang, Q. Zhang, W. Chen, Y. Gu, Q. Chen, Inorganic chemistry, 2019, 58, 3564.
[20] E. Zare, Z. Rafiee, Applied Organometallic Chemistry, 2020, e5516.
[21] S. Wang, M. Wahiduzzaman, L. Davis, A. Tissot, W. Shepard, J. Marrot, C. Martineau-Corcos, D. Hamdane, G. Maurin, S. Devautour-Vinot, Nature communications, 2018, 9, 1.
[22] M. Wahiduzzaman, S. Wang, B.J. Sikora, C. Serre, G. Maurin, Chemical Communications, 2018, 54, 10812.
[23] D. Lv, J. Chen, K. Yang, H. Wu, Y. Chen, C. Duan, Y. Wu, J. Xiao, H. Xi, Z. Li, Chemical Engineering Journal, 2019, 375, 122074.
[24] Y. Dou, H. Zhang, A. Zhou, F. Yang, L. Shu, Y. She, J.-R. Li, Industrial & Engineering Chemistry Research, 2018, 57, 8388.
[25] K. Epp, A.L. Semrau, M. Cokoja, R.A. Fischer, Chem. Cat. Chem, 2018, 10, 3506.
[26] H. Suzuki, O. Tomita, M. Higashi, R. Abe, Journal of Materials Chemistry A, 2017, 5, 10280.
[27] S.R. Mandha, S. Siliveri, M. Alla, V.R. Bommena, M.R. Bommineni, S. Balasubramanian, Bioorganic & medicinal chemistry letters, 2012, 22, 5272.
[28] D. Armesto, W.M. Horspool, N. Martin, A. Ramos, C. Seoane, The Journal of Organic Chemistry, 1989, 54, 3069.
[29] M. Heravi, A. Ghods, F. Derikvand, K. Bakhtiari, F. Bamoharram, Journal of the Iranian Chemical Society, 2010, 7, 615.
[30] R.H. Vekariya, K.D. Patel, H.D. Patel, Research on Chemical Intermediates, 2016, 42, 4683.
[31]H. Chavan, D. Survase, S. Dongare, V. Helavi, S. Ganapure, Iranian Chemical Communication, 2017, 5, 105.

[32]S.R. Mandha, S. Siliveri, M. Alla, V.R. Bommena, M.R. Bommineni, S. Balasubramanian, Bioorganic & medicinal chemistry letters, 2012, 22, 5272.
[33]H. Kiyani, H. Samimi, F. Ghorbani, S. Esmaieli, Current Chemistry Letters, 2013, 2, 197.

[34]M. Heravi, A. Ghods, F. Derikvand, K. Bakhtiari, F. Bamoharram, Journal of the Iranian Chemical Society, 2010, 7, 615.

[35] F. Sevgi, A.D. Bedük, Synthesis and antimicrobial activity of novel glyoximes containing quinoline moiety, World Appl. Sci. J. 19 (2) (2012) 192.

[36] H. B' Bhatt, S. Sharma, Synthesis and antimicrobial activity of pyrazole nucleus containing 2-thioxothiazolidin-4-one derivatives, Arab. J. Chem. 10 (2017) S1590.

[37] J. Kutkowska, B. Modzelewska-Banachiewicz, G. Zi, W.R. Kowska, T. Urbanik- Sypniewska, Z. Zwolska, et al., Antimicrobial activity of 3,4-disubstituted- 1,2,4-triazole derivatives, Membranes 62 (4) (2005) 303.

[38] S.M.H. Nasrollahi, M.A. Ghasemzadeh, M.R. Zolfaghari, Synthesis and antibacterial evaluation of some new 1,4-dihydropyridines in the presence of Fe_3O_4@ silica sulfonic acid nanocomposite as catalyst, Acta Chim. Slov. 65 (1) (2018) 199.

[39] P. Mehta, P. Verma, Antimicrobial activity of some derivatives of 1,4- dihydropyridines, J. Chem. 2013 (2012).